New Zealand Journal of Geology & Geophysics, 2003, Vol. 46: 95–106
0028–8306/03/4601–0095 $7.00/0 © The Royal Society of New Zealand 2003

Radiocarbon and luminescence dating of overbank deposits in outwash sediments of the Last Glacial Maximum in North Westland, New Zealand

ANNE HORMES*
Institute of Geological Sciences
Universität Bern
Baltzerstrasse 1
CH0-3012 Bern, Switzerland
email: anne.hormes@angstrom.uu.se

FRANK PREUSSER
Institute of Geological Sciences
Universität Bern
Baltzerstrasse 1
CH-3012 Bern, Switzerland
email: preusser@geo.unibe.ch

GEORGE DENTON
Department of Geological Sciences
5790 Bryand Global Sciences Center
University of Maine
Orono, Maine 04469-5790, USA

IRKA HAJDAS
Institute of Particle Physics
ETH Hönggerberg
HPK, CH-8093 Zürich, Switzerland

DOMINIK WEISS
Imperial College of Science, Technology and Medicine
Department of Earth Sciences and Engineering
Prince Consort Road
London SW7 2BP, UK

THOMAS F. STOCKER
Climate and Environmental Physics
Universität Bern
Sidlerstrasse 5
CH-3012 Bern, Switzerland

CHRISTIAN SCHLÜCHTER
Institute of Geological Sciences
Universität Bern
Baltzerstrasse 1
CH-3012 Bern, Switzerland

*Present address: Ångströmlaboratoriet, Uppsala University, Box 534, SE-751 21 Uppsala, Sweden.

G01023; published 21 March 2003
Received 25 July 2001; accepted 21 November 2002

Abstract In the Grey River valley, North Westland, New Zealand, extensive terraces of outwash sediments assigned to the Otira glaciation form outstanding geomorphologic features. Four layers of organic sediments subdivide stratified outwash gravels of the major terrace. The age of the fine-grained sediments is constrained by 55 radiocarbon (^{14}C) ages and 8 optically stimulated luminescence (OSL) ages. The calibrated radiocarbon ages cover the age range between 21 350 and 23 890 cal yr BP. The ages for each different layer are consistent and are in stratigraphic order with mean ages of 22 350 cal yr BP (layer A), 22 470 cal yr BP (layer B), 22 930 cal yr BP (layer C), and 22 960 cal yr BP (layer D).

OSL dating of the silty overbank deposits alternating with the organic beds imply a deposition at 21 700 ± 2600 yr. The use of different organic compounds for radiocarbon dating (separated organic residues, humic acids, terrestrial seeds) and the consistency with the luminescence dating support the reliability of the results. We use the informal name Raupo complex for the overbank deposits and consider it to reflect a moderate climate oscillation between two glacial advances during Oxygen Isotope Stage 2.

Keywords Last Glacial Maximum; radiocarbon; luminescence; fluvial sediments; New Zealand

INTRODUCTION

Climate evolution during the last glacial period is well documented in Greenland and Antarctic ice core records (Neftel et al. 1988; Johnson et al. 1992; Dansgaard et al. 1993) as well as in deep sea sediment sequences (e.g., Nelson et al. 1993). In contrast, terrestrial records of small scale climate variations during the Last Glacial Maximum (LGM), in particular from the Southern Hemisphere, are rare. Radiocarbon ages suggest that, during the LGM, mountain glaciers expanded at the same time in Tasmania, New Zealand, and Chile (Gillespie & Molnar 1995; Denton et al. 1999).

Today, the South Island of New Zealand is in the zone of the Southern Westerlies, which dominate the climate south of the Subtropical Front (STF). This belt of zonal western airflow extends south from c. 30°S in July and 40°S in January to the Antarctic Trough of low pressure (a cyclonic stagnation, which fluctuates between 60 and 72°S; Barry & Chorley 1998). During the LGM, this belt of westerly airflow shifted northwards by at least 5° latitude (Nelson et al. 1993). A decrease in temperatures over the Southern Alps caused a drop in snowline elevation on the South Island of New Zealand, which triggered the glacier advances of the LGM. Precise dating of the LGM and of associated secondary glacier oscillations is a prerequisite for understanding the paleoclimate linkage between Antarctica, the Southern Ocean, and terrestrial records of New Zealand.

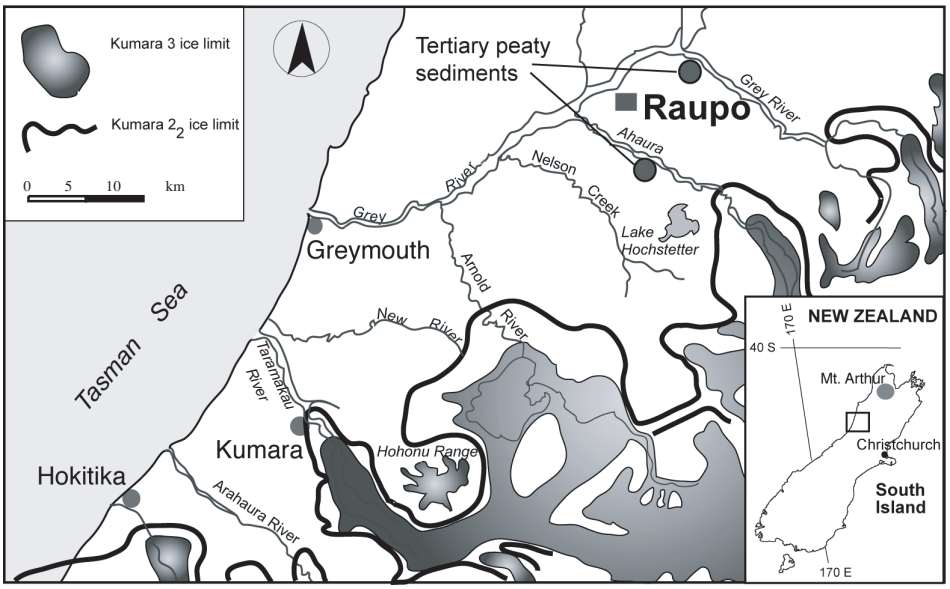

Fig. 1 Location of the Raupo study area. Kumara-2_2 and -3 ice limits according to Suggate (1965) and Suggate & Moar (1969). *Inset*: Outline map of the South Island of New Zealand.

Several glacial pulses during the Otira glaciation, the last glaciation in New Zealand, are recognised on the basis of moraines and outwash gravel terraces (Pillans et al. 1993). Three advances for the last glaciation are described in Westland (Suggate 1990) and five in Fiordland (Williams 1996). Their chronostratigraphic positions are based on only a few radiocarbon and U/Th ages. The three advances recognised in Westland are named Kumara-2_1, assigned to Oxygen Isotope Stage (OIS) 4, Kumara-2_2 and Kumara-3, which occurred during OIS 2 (Suggate 1990) (Fig. 1). The Kumara-2_2 glacial pulse was radiocarbon dated at older than 22 300 ± 350 yr BP (Suggate & Moar 1970). Two ages of 18 750 ± 180 and 18 600 ± 290 yr BP on organic silts between Kumara-2_2 and Kumara-3 outwash deposits suggest a moderate climate interval (Suggate 1965; Suggate & Moar 1970). The Kumara-3 glacial advance occurred after 16 450 yr BP, and is the last major advance to the lowlands (Suggate 1990). The validity of radiocarbon ages from the South Island sites, especially from Westland, is debated because of potential contamination (Hammond et al. 1991). Here, we show that radiocarbon dating is suitable to refine the chronostratigraphy in terrestrial sequences of New Zealand by using appropriate materials and techniques. Different chemical treatment methods were applied to the organic material to check possible contamination of the samples with young humic acids or reworked older material (Mook & Streurman 1983; Olsson 1986).

We present a set of radiocarbon and luminescence ages on organic material and on silt in a relict overbank sequence at Raupo, a site first described by Suggate (1965). The section is located in the Raupo gravel pit in the Grey River valley in North Westland, South Island of New Zealand, at 42°19′S, 171°35′E (Fig. 1).

GEOLOGIC SETTING

The terrace of the Totara Flat was accumulated during the Otira glaciation as an extensive outwash fan. The headwaters of the Grey River are in the Southern Alps and the coastal Paparoa Range, both of which are composed of greywackes and granitic intrusions. In the drainage area of the Grey River, some peaty deposits are common within conglomerate deposits (Fig. 1). For example, in Findlay Creek, tributary of Nelson Creek, the peaty deposits are situated at the base of the Old Man Gravels, associated with the Ross glaciation (Suggate pers. comm.). In addition, contamination of radiocarbon samples by old carbon is, therefore, possible in the Grey River valley. Coal beds of the upper Miocene–Pliocene have been observed in the areas shown in Fig. 1.

The surface of the Totara Flat is 96–98 m a.s.l.; the bottom of the gravel pit is 73 m a.s.l. Organic layers with the top at 88 m a.s.l. in fine-grained overbank sediments conformably overly the Kumara-2_2 outwash gravels. The top of the fine-grained silty overbank sediments is partially eroded by the Kumara-3 meltwater stream. The Kumara-3 advance is younger than 16 450 yr BP (following published data in Suggate (1990) and Denton et al. (1999)). The changes in sedimentation are interpreted as changes in fluvioglacial dynamics caused by re-adjusted glacier movements and meltwater drainage.

We have studied five sections (I–IV and VI) at Raupo West within the same outcrop (Fig. 2). Section Raupo East (V) is located 200 m east of the Raupo gravel pit (Fig. 3). These sections contain well-defined organic layers of 2–10 cm thickness, which intercalate with silty clay to silty sand beds. The grey clayey silts contain seeds of Cyperaceae and Gramineae, while the brown organic mud contains Herbaceae pollen (Suggate & Moar 1970). The overbank deposit with its organic layers from both sections is informally named the Raupo complex.

GEOCHEMICAL ANALYSIS

Geochemical analyses were carried out for characterisation of the organic sediments and for an assessment of influencing factors on the measured ages. Br, Fe, and Rb were measured directly in the dry, solid samples using EMMA miniprobe XRF at the Institute of Geological Sciences, Ukrainian

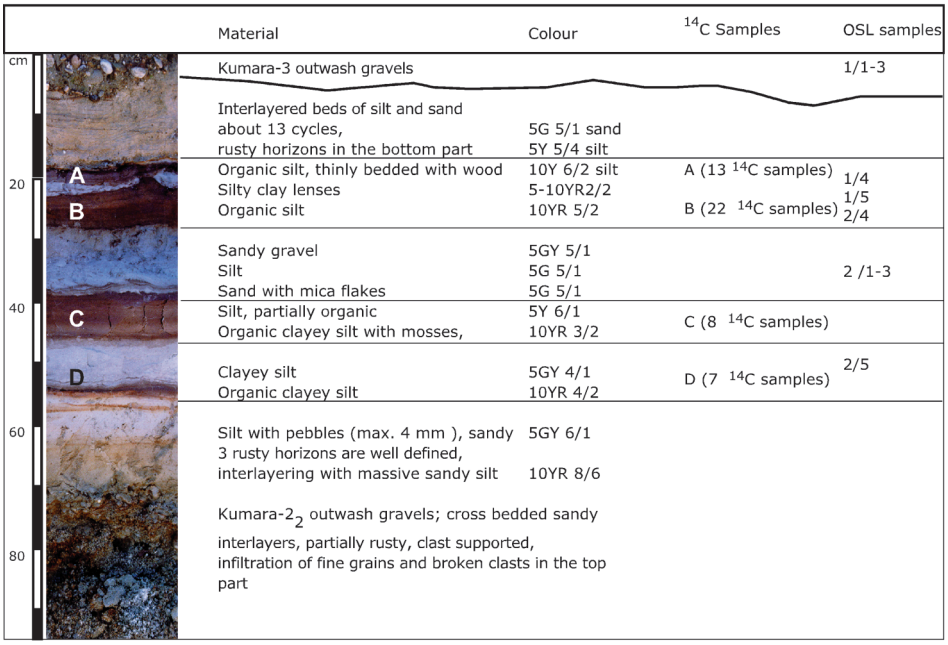

Fig. 2 Composite lithostratigraphy of the Raupo gravel pit with five sections (I, II, III, IV and VI) combined as Raupo West. Sedimentology and thickness of the sediment units are shown. Samples mentioned in the text are indicated. Layers A, B, C, D are the organic layers.

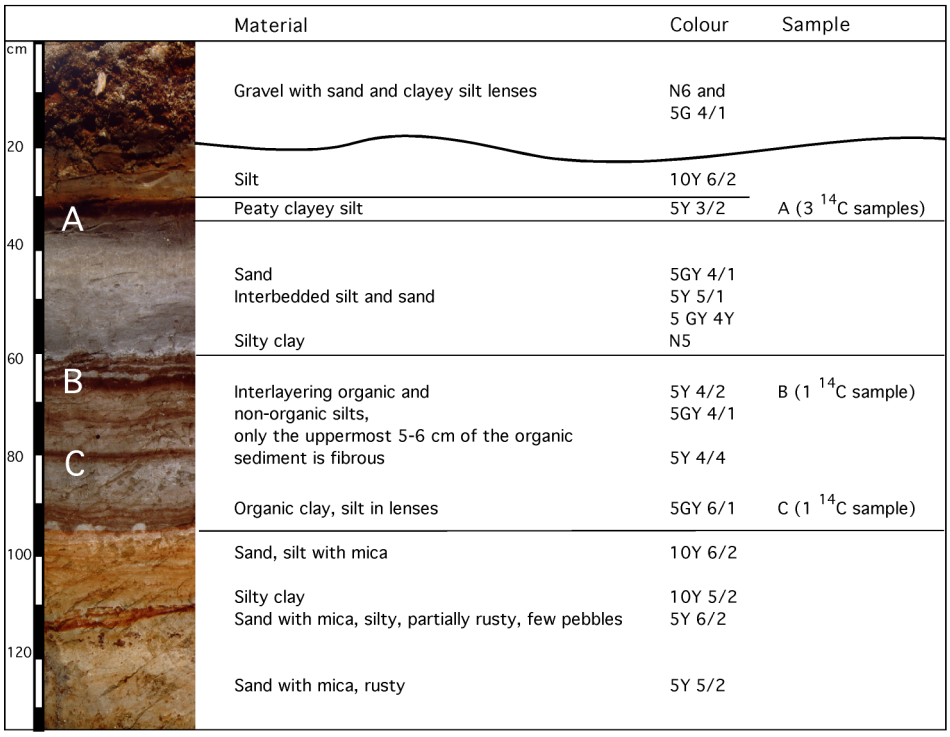

Fig. 3 Lithostratigraphy of the Raupo East section (Raupo V). The correlation of the organic layers with the Raupo West sections is provisionally labelled as A, B, C.

Academy of Science, Kiev. The set-up of the instrument and analytical details are given in Cheburkin & Shotyk (1996) and Weiss et al. (1998). The minimum detection limits for all these elements were well below the smallest measured concentrations (Table 1). The precision of the elemental analyses was c. 30% for concentrations of c. 1 ppm, 10% for 10 ppm, and 6% for 60 ppm. Analytical accuracy was determined by multiple measurements of the certified plant material—apple leaves (NBS 1515), peach leaves (NBS 1547), and pine needles (NBS 1575)—and was within ±12% for all elements.

RADIOCARBON DATING

Conventional radiocarbon ages of organic sediments were obtained from pretreated organic residues and humic acids to exclude dating a mixture of organic material derived from a variety of sources (e.g., Andrée et al. 1986; Goh et al. 1978;

Mook & Streurman 1983). The extracted humic acids were dated to check if the bulk samples were contaminated with infiltrated younger humic acids (Kigoshi et al. 1980). These measurements were carried out at the Radiocarbon Laboratory, Environmental Physics at University of Bern, using low activity Cu proportional β-counters filled with CH_4 (Fairhall et al. 1961). Screening techniques and the proportional gas counting method have been described by Loosli et al. (1980).

Dating of terrestrial plant macrofossils avoids problems with any possible contamination with reworked material in bulk samples and reservoir effects (Andrée et al. 1986; Zbinden et al. 1989; Hajdas 1993). Such reservoir effects occur because aquatic plants partially assimilate $^{14}CO_2$ from groundwater. Therefore, we exclusively dated the seeds of terrestrial plants (Cyperaceae, Juncaceae) with the Accelerator Mass Spectrometer (AMS) facility at the ETH/PSI in Zürich (Bonani et al. 1987). Subsamples of humic acid sample 31-III-c were dated in Bern and in Zürich to check possible age deviations due to different laboratory and measurement procedures. The results are given in Tables 2 and 3; the sample measured with AMS gave an age of 18 790 ± 130 yr BP, whereas the conventionally dated sample is 19 328 ± 148 yr BP. Also, the stable isotope ratio is different for these two subsamples ($^{13}C = –27.8‰$ and –31.0‰, respectively). This might be a hint for a slightly different composition of the two subsamples. However, the radiocarbon age calibration curve confirms the existence of a plateau during this time (Stuiver et al. 1998). Therefore, we conclude that the uncalibrated data should not be overestimated because the calibrated ages show overlapping data ranges, thus confirming the comparability of both laboratories.

Laboratory storage and chemical treatment

The samples were stored in the refrigerator at 3–4°C in slightly acidified water following recommendations by Törnqvist et al. (1992) to avoid contamination with fungal growth and/or bacteria (Geyh et al. 1974). Extracted seeds were stored at –18°C in acidified water for less than 2 months (Wohlfarth et al. 1998).

Organic residue samples

Bulk sediment samples were chemically treated to remove contamination by younger humic acids. Standard treatment of organic sediments consisted of two acid and two alkali steps: the samples were soaked in NaOH (2% v/v) overnight in order to remove humic and fulvic acids. HCl (4% v/v) was then used to remove carbonate, metal ions, hydrous oxides, and hydrated silicate minerals. Treatment with HCl also removes atmospheric CO_2, which might have been adsorbed during the alkaline treatment (Goh et al. 1978; Hammond et al. 1991). The extracts of acid and alkaline treatments were separated from the residue and removed in solution. After each chemical step the samples were washed with deionised water until pH 7 was reached.

Humic acid

Separation of humic and fulvic acids was achieved by dissolving the samples in NaOH solution. After addition of HCl or H_2SO_4 to the humic acids, "flakes" which formed were consequently separated from the solution by centrifugation at 3000 rpm and washed with deionised water until pH 7 was reached (Kigoshi et al. 1980).

Plant macrofossils

Terrestrial plant macrofossils were separated from bulk sediments by washing with deionised water and soaking overnight in NaOH (2% v/v). After another washing step with deionised water, samples were left in HCl (4% v/v) overnight and then washed again. The samples were wet sieved (400 µm mesh) and macrofossils (seeds) were carefully extracted with tweezers. Between 2.8 and 8.2 mg of macrofossils were evacuated and then combusted for 2 h at 950°C. Reference seeds were dried and photographed. We exclusively dated Cyperaceae and Juncus seeds because both species assimilate atmospheric CO_2 only (White et al. 1994).

Calibration of radiocarbon ages

There are two methods to convert radiocarbon ages (expressed as "yr BP") to calendar years (expressed as

Table 1 Geochemical data of the organic layers and the fine-grained overbank deposits.

Horizon	Ash % α	pH β	$CaCO_3$ % χ	Rb ppm δ	Fe ppm δ	Br ppm δ	%C of bulk sed. γ	%C of humic acid γ
A	76.5	4.42	0.05	91.5	15416	15.4	8.4	37.3
B	67.7	4.44	0.07	60.3	10479	27.2	8.3	23.0
C	69.5	4.66	0.07	57.9	7743	23.9	13.9	23.2
D	89.4	4.57	0.05	91.3	27549	7.7	9.7	22.8
average	75.8	4.52	0.06	75.3	15297	18.5	10.08	26.6
silt A-B	91.8	4.34	0.04	115.6	21778	4.0	n.d.	n.d.
silt B-C	92.4	4.49	0.03	110.0	21014	4.0	n.d.	n.d.
silt C-D	93.3	4.86	0.08	98.9	22606	1.0	n.d.	n.d.
sand beneath	97.7	4.90	n.d.	n.d.	n.d.	n.d.	n.d.	n.d.
average	93.8	4.56	0.05	108.2	21799	3.0	n.d.	n.d.

n.d. not determined.
α based on loss on ignition at 550°C using 1.5 g sample weight.
β measured in 0.1*M* KCl solution.
χ measured in the ash with the Coulomat CS-mat 5500 (Ströhlein GmbH & Co. Kaarst, Germany) at 1300°C under N_2 supply.
δ measured directly in the dry, solid samples using EMMA miniprobe XRF.
γ measured on the CO_2 gas with a mass spectrometer after pyrolysis.

"cal yr BP") in the time range discussed here. The CALIB 4.1 program by Stuiver & Reimer (1999) is based on uranium-thorium (U-Th) ages of 10 corals (Bard et al. 1998). Another method of calibration is to use the dataset from Japanese Lake Suigetsu by Kitagawa & van der Plicht (1998). The ^{14}C chronology of these varved lake sediments is based on ages of 43 terrestrial macrofossils between 14 999 and 24 010 cal yr BP. This dataset is not yet incorporated into the INTCAL 98-calibration curve, which extends to 24 000 cal yr BP (Stuiver et al. 1998). Using the Suigetsu calibration will increase the calibrated ages by 1.6%. For our data we have used the CALIB 4.1 1999 software with 1σ standard deviation. Calibration is necessary to allow a direct comparison with luminescence ages; radiocarbon ages are not calender years owing to radiocarbon production variations, whereas luminescence ages represent calendar years.

Results and discussion of the ^{14}C ages

A total of 55 radiocarbon ages were obtained from the organic sediment layers of the Raupo complex (Tables 2, 3;

Table 2 Radiocarbon ages for the Raupo West sections. Calibrated ages are calculated using CALIB 4.1 program of Stuiver & Reimer (1999) based on the dataset of Stuiver et al. (1998).

NZ code	Lab code	Material	^{13}C	^{14}C yr BP	cal BP, 1σ
Organic layer A					
6-II a	B-6862	humic acid	–30.9	18316 ± 211	22180–21350
59-VI a	B-7199	organic residue	–31.8	18780 ± 65	22660–21950
55-IV a	B-6404	organic residue	–31.0	18788 ± 110	22680–21940
1-I a	B-6861	humic acid	–29.4	18813 ± 123	22710–21960
63-VI a	B-7203	organic residue	–30.0	18828 ± 65	22710–22000
1-I a	B-6861	organic residue	–30.4	18857 ± 67	22750–22030
61-VI a	B-7201	organic residue	–29.1	18899 ± 73	22800–22080
64-VI a	ETH-19605	seeds	–27.6	18910 ± 130	22830–22070
50-IV a	B-6398.1	organic residue	–29.7	18912 ± 80	22810–22090
58-VI a	B-7207	organic residue	–29.6	18924 ± 100	22840–22100
6-II a	B-6862	organic residue	–30.6	18938 ± 103	22850–22110
64-VI a	B-7205	organic residue	–29.6	18952 ± 73	22860–22140
51-IV a	B-6398.2	organic residue	–31.3	19967 ± 130	[24080]–23250
Organic layer B					
13-III b	B-6849	humic acid	–32.2	18627 ± 121	22490–21750
44-II b	ETH-19608	seeds	–25.1	18680 ± 150	22570–21800
34-II b	B-6875	humic acid	–30.0	18715 ± 102	22590–21860
43-II b	B-6847	organic residue	–29.7	18778 ± 102	22660–21930
43-II b	B-6847	humic acid	–31.0	18876 ± 120	22790–22040
61-VI b	B-7202	humic acid	–29.9	18887 ± 72	22780–22070
63-VI b	ETH-19611	seeds	–25.9	18890 ± 130	22810–22050
61-VI b	ETH-19604	seeds	–28.7	18890 ± 130	22810–22050
13-III b	B-6849	organic residue	–30.0	18893 ± 66	22790–22070
59-VI b	B-7200	organic residue	–30.1	18926 ± 104	22810–22080
44-II b	B-6846	humic acid	–30.9	18939 ± 110	22860–22110
66-V b	B-7195.1	humic acid	–30.3	18940 ± 231	22900–22100
35-II b	ETH-19609	seeds	–27.0	18950 ± 150	22890–22110
34-II b	B-6875	organic residue	–32.4	18967 ± 107	22890–22140
64-VI b	ETH-19610	seeds	–29.1	18980 ± 130	22910–22150
63 VI b	B-7204	organic residue	–31.1	18981 ± 73	22890–22170
64-VI b	B-7206	organic residue	–31.1	19003 ± 80	22920–22190
59-VI b	ETH-19607	seeds	–28.0	19010 ± 130	22950–22180
61-VI b	B-7202	organic residue	–30.1	19067 ± 73	23000–22270
35-II b	B-6876	organic residue	–30.1	19111 ± 110	23060–22300
44-II b	B-6846	organic residue	–30.3	19137 ± 90	23080–22340
35-II b	B-6876	humic acid	–30.2	19252 ± 133	23240–22450
Organic layer C					
31-III c	ETH-19602	humic acid	–27.8	18790 ± 130	22690–21930
31-III c	B-6929	humic acid	–28.7	19244 ± 70	23210–22470
54-IV c	B-6403	organic residue	–30.7	19280 ± 110	23260–22490
32-III c	B-6850	humic acid	–31.0	19328 ± 148	23340–22530
52-IV c	B-6400.1	organic residue	–30.4	19400 ± 80	23400–22640
32-III c	B-6850	organic residue	–32.2	19462 ± 70	23470–22710
14-I c	B-6932	humic acid	–30.5	19502 ± 92	23520–22750
53-IV c	B-6400.2	organic residue	–30.5	19563 ± 80	23590–22820
Organic layer D					
57-IV d	B-6407.2	organic residue	–30.7	18671 ± 100	22540–21810
22-III d	B-6930	humic acid	–30.4	19349 ± 240	23420–22500
58-IV d	B-6407.3	organic residue	–30.8	19533 ± 140	23580–22770
21-I d	B-6851	organic residue	–33.0	18934 ± 230	22920–22040
20-I d	B-6928	humic acid	–32.3	19590 ± 131	23640–22830
21-I d	B-6851	humic acid	–30.1	19590 ± 240	23700–22770
56-IV d	B-6407.1	organic residue	–30.3	19800 ± 130	23890–23070

Fig. 2, 3). Statistical χ^2-tests based on calibrated ages were carried out for the different organic layers, assuming normal distribution according to Geyh (1983).

Each layer forms a distinct group of age cluster. In the whole radiocarbon dataset, only one sample of layer A is not consistent with the other samples (51-IV-a; Table 2) and thus is rejected for calculations of mean ages.

Ages for layer A range between 21 350 and 22 860 cal yr BP; for layer B between 21 750 and 23 240 cal yr BP; for layer C between 21 930 and 23 590 cal yr BP; and for layer D between 21 810 and 23 890 cal yr BP. The mean ages for each layer are 22 350 cal yr BP (layer A), 22 470 cal yr BP (layer B), 22 930 cal yr BP (layer C), and 22 960 cal yr BP (layer D).

Fourteen bulk samples were divided into subsamples and dated separately to compare the results of organic residue with humic acid and seeds. This procedure allows the detection of possible contamination by younger humic acids, dissolution of old carbonate, and reworked older organic material (described as crucial for Westland by Hammond et al. (1991)).

Comparison of the subsamples confirmed the reliability of sample treatment and measurements (Fig. 4). Only three samples (6-II-a, 21-I-d, and 51-IV-a) indicated a possible low-level contamination. We consider the following possibilities to account for these minor age deviations:

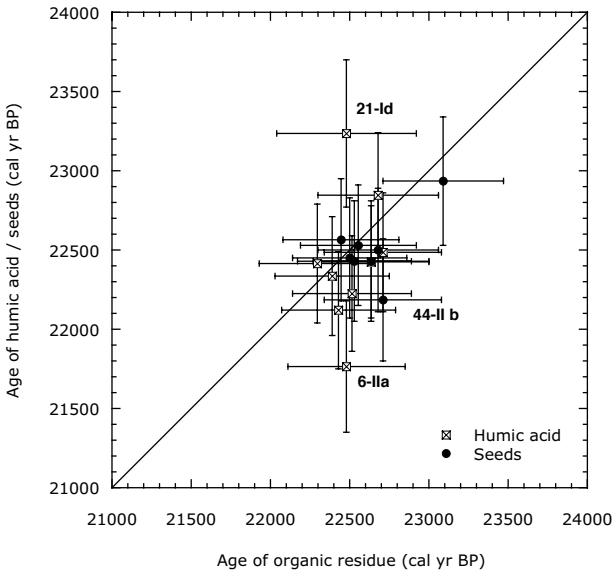

Fig. 4 Comparison of radiocarbon ages of subsamples from seeds, organic residues after base-acid-base-acid-pretreatment, and humic acids taken from 14 bulk samples.

(1) Contamination of samples by reworked older organic material

The significant greater age of sample 51-IV-a in layer A might have been caused by reworked organic material. In the Great River catchment area, we observed Tertiary peat layers up to 1.5 m thick, which were under active erosion by the river.

(2) Influence of groundwater

The humic acid of sample 21-I-d of layer D is slightly older than the corresponding organic residue. One explanation for the slightly older age is the possible contamination of older humic acids dissolved in groundwater. The increasing ash from the top layer to the bottom layer throughout the section indicates a decreasing percentage of organic substance due to groundwater processes. The increasing element concentration of iron from layer C to D (Table 1) also underlines a groundwater influence within layer D. As well, the Rb concentration increase in layer D implies further groundwater as source and is a possible contamination factor for sample 21-I-d. However, there is no evidence of strong groundwater influence throughout the complete section: for example, the Rb/ash ratios in all four organic layers A–D vary between 0.83 and 1.20 and agree well with the silt layers inbetween with Rb/ash ratios of between 1.06 and 1.26.

(3) Translocation of humic acids

The humic acid of sample 6-II-a is slightly younger than the corresponding organic residue possibly due to infiltration of younger humic acids. Fe/ash ratios are different in all four organic layers, ranging between 111 in layer C and 308 in layer D, while all the silt layers show a similar Fe/ash ratio of 227 to 242. This suggests a strong Fe mobility within the organic layers due to the high redox potential and the presence of organic substances. This is typical for soils formed in sediments under anaerobic and acidic environments, because enhanced reduction of Fe is associated with strong complexation with organic ligands and increased mobility of Fe-org complexes (Steinmann & Shotyk 1997). The significant Fe enrichment in layer D is related to chemical weathering processes, because rusty Fe-horizons have been observed in the field (Fig. 2, 3). The slightly higher Fe/ash ratio in layer A might well be explained by a migration of Fe associated with migration of organic material (Sposito 1989). Therefore, infiltration seems only to have affected

Table 3 Radiocarbon ages for the Raupo East section. Calibrated ages are calculated using CALIB 4.11999 program of Stuiver & Reimer (1993) based on the dataset of Stuiver et al. (1998).

NZ code	Lab code	Material	^{13}C	^{14}C yr BP	cal BP (1 σ)
Organic layer A					
66-V a	B-7195	organic residue	–30.8	18428 ± 170	22280–21500
67-V a	B-7196	organic residue	–25.1	18510 ± 180	22390–21590
66-V 1	B-7073.1	humic acid	–29.3	18940 ± 230	22920–22050
Organic layer B					
66-V b	B-7195.1	humic acid	–30.3	18940 ± 231	22900–22100
Organic layer C					
68-V b	B-7197	organic residue	–29.8	19224 ± 80	22990–22320

layer A, possibly because the overlying gravels have a higher permeability. Therefore, we consider this hypothesis of migrating organic material as the most probable contamination for samples 6-II-a and 51-IV-a.

LUMINESCENCE DATING

Aitken (1985, 1998), Prescott & Robertson (1997), and Wintle (1997) discuss the physical background and methodological aspects of luminescence dating in detail. The opportunity to apply radiocarbon and luminescence dating in the same stratigraphic unit is an important crosscheck. In this study, infrared stimulated luminescence (IRSL), green light stimulated luminescence (GLSL), and thermoluminescence (TL) were used to date four samples of silty layers from the Raupo complex (section VI, Fig. 2) resulting in eight ages. The main advantage of optical dating is the higher light sensitivity of the luminescence signal. Bleaching experiments and fading tests were carried out for characterising the physical properties of the luminescence signals.

Equivalent dose determination (ED)

All sample preparation was done under subdued red light laboratory illumination. The samples that are listed in Table 4 were prepared using the fine grain technique of Frechen et al. (1996) and standard chemical treatments (HCl, Na-oxalate, H_2O_2). Irradiation was carried out using a ^{60}Co source (additive dose method) applying seven dose groups, five aliquots each. After irradiation, the samples were stored for at least 4 weeks at room temperature and subsequently heated to 150°C for 16 h to remove unstable components of the luminescence signal. The non-light sensitive TL signal was defined as the remaining TL after 16 h of exposure to an Osram Ultra-Vitalux UV lamp (300 W). Luminescence measurements were performed using a Risø TL-DA 12 reader equipped with IR-diodes and a green light source (Bøtter-Jensen et al. 1991; Bøtter-Jensen & Duller 1992). A violet-blue filter set (Schott BG39, Corning 7-59) was used for the IRSL/TL and a UV transmitting filter (Hoya U340) for the GLSL/TL readout. Since the samples contain c. 7% K-felspar, as analysed by XRF, these signals are dominated by emissions from this mineral (Krbetschek et al. 1997). OSL was recorded during a 60 s shinedown of IR diodes (IRSL) and green light (GLSL), respectively. The integral 50–60 s was subtracted as late-light from the rest of the shinedown curves to avoid machine background and slow-to-bleach components (Aitken & Xie 1992). Luminescence ages were calculated on the basis of the growth curves using the integral 0–25 s (OSL) and 250–450°C (TL), respectively.

Dose rate determination

The contents of dose rate relevant elements were determined by high resolution gamma spectrometry (Preusser & Kasper 2001). Water contents were estimated on the basis of the actual water content of the samples. A cosmic dose rate of 150 ± 20 μGy yr^{-1} (Aitken 1985) and a-values of 0.07 ± 0.02 (OSL) and 0.08 ± 0.02 (TL) were used (Preusser 1999a). The radioactivity data and resulting dose rates are summarised in Table 5.

Inhomogeneous "bedded" sedimentary environments, such as at Raupo, provide a possible error source because of variability in γ-dose rate of the single horizons (Brennan et al. 1997). Therefore, additional samples, which were not dated, were taken from above and below the layers sampled for luminescence dating to determine the dose rate and mineralogical content (Table 5). The lower samples (RPO 2/3–5) show only small variations in the calculated dose rate, which corresponds to a homogeneous γ-irradiation field. Some higher variations in the dose rate were calculated for

Table 4 Radioactivity data and resulting dose rates for luminescence dating from additional samples above and below the dated samples. The luminescence samples 1/4, 2/4, and 2/5 are organic samples, which have been sampled from the radiocarbon-dated horizons.

Sample	K (%)	Th (ppm)	U (ppm)	W (%)	D_{IRSL} (Gy ka^{-1})	D_{TL} (Gy ka^{-1})
RPO 1/3	2.09 ± 0.10	13.93 ± 0.70	3.80 ± 0.19	25 ± 5	4.3 ± 0.4	4.4 ± 0.4
RPO 1/4	1.85 ± 0.09	10.33 ± 0.50	2.57 ± 0.13	25 ± 5	3.3 ± 0.3	3.4 ± 0.3
RPO 1/5	1.27 ± 0.06	13.89 ± 0.69	3.54 ± 0.18	25 ± 5	3.5 ± 0.3	3.7 ± 0.4
RPO 2/3	1.77 ± 0.08	15.66 ± 0.78	4.27 ± 0.21	30 ± 5	4.0 ± 0.4	4.2 ± 0.5
RPO 2/4	1.92 ± 0.09	15.32 ± 0.77	4.00 ± 0.20	30 ± 5	3.9 ± 0.4	4.0 ± 0.4
RPO 2/5	1.38 ± 0.07	18.98 ± 0.95	3.77 ± 0.19	30 ± 5	3.9 ± 0.4	4.0 ± 0.5

Table 5 Equivalent dose estimates and luminescence ages for the silty layers from the Raupo section VI. 1/1–3 is from above all organic layers and 2/1–3 is a silty layer between organic layers B and C (cf. Fig. 2).

Sample	ED_{OSL} (Gy)	Age_{OSL} (ka)	ED_{TL} (Gy)	Age_{TL} (ka)
RPO 1/1 IR	110.5 ± 1.6	26.0 ± 3.8	195.7 ± 27.1	44.5 ± 7.7
RPO 1/1 GL	99.5 ± 16.5	23.4 ± 4.6	234.8 ± 35.2	53.4 ± 9.7
RPO 1/2 IR	107.2 ± 7.1	25.2 ± 3.1	244.3 ± 68.3	55.6 ± 10.0
RPO 1/2 GL	96.8 ± 4.1	22.8 ± 2.5	203.1 ± 6.9	46.2 ± 4.2
RPO 2/1 IR	80.9 ± 5.8	20.2 ± 2.7	146.5 ± 14.1	35.2 ± 5.1
RPO 2/1 GL	75.1 ± 3.1	18.7 ± 2.2	148.5 ± 14.0	35.7 ± 5.2
RPO 2/2 IR	88.1 ± 4.5	22.6 ± 2.7	160.0 ± 17.5	38.5 ± 5.9
RPO 2/2 GL	80.3 ± 5.5	20.0 ± 2.6	185.9 ± 19.8	44.7 ± 6.8

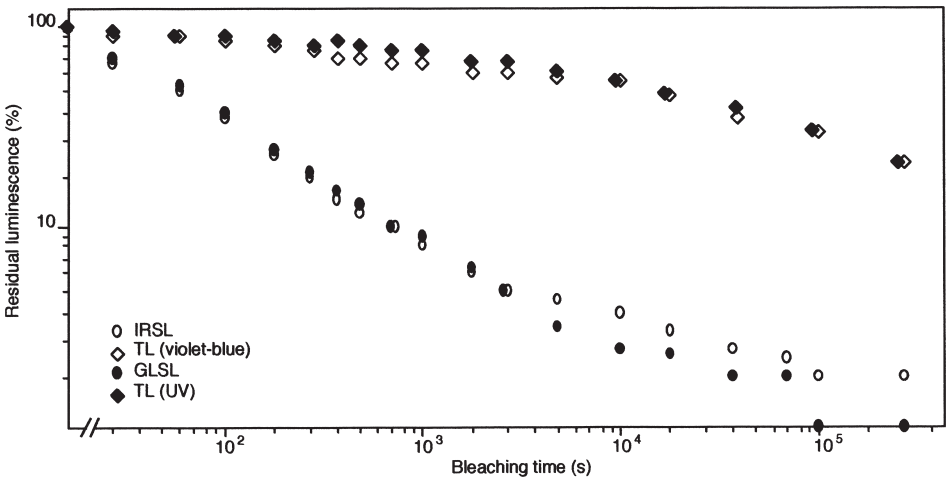

Fig. 5 Residual luminescence after indicated bleaching time for a range of luminescence emissions.

sample RPO 1 (Tables 4, 5). The difference in γ-dose rate of samples RPO 1/3 and RPO 1/4 is 0.3 Gy ka^{-1} which is 7% of the total dose rate. However, since most of the γ-irradiation will originate from the sampled horizon, a significant underestimation (>1%) of the total dose rate due to an inhomogeneous γ-irradiation field is unlikely.

Zeroing of the luminescence signal

The prerequisite for dating is the complete bleaching of the luminescence signal before deposition. Sediment grains undergoing fluvial transport are, in comparison to aeolian deposits, less well-exposed to sunlight due to attenuation of light penetration by turbidity, turbulence, and water depth (Ditlefsen 1992). Therefore, resetting of the luminescence signal has to be verified (e.g., by the use of shine plateau tests; Huntley et al. 1985). A shine plateau is present when the paleodose is constant over the whole stimulation time, although the suitability of these tests is controversial (Aitken 1992).

Zeroing of the luminescence before deposition is also indicated by corresponding OSL and TL age estimates since both signals show significant differences in their bleaching characteristics (Duller 1992; Preusser et al. 2001). This approach, however, negates the advantage of OSL, the easy-to-bleach nature of the signal, and will thus be limited to well-bleached sediments.

It has been suggested that the comparison of OSL from quartz and feldspars (Fuller et al. 1994) and of different IRSL emissions (Krause et al. 1997) might be appropriate methods to identify insufficient bleaching. However, no significant differences in the resetting characteristics of several OSL signals have been found (Preusser 1999b,c). Other studies imply a less rapid bleachability of the GLSL in comparison to IRSL from feldspars and polymineral fine grain assemblages (Spooner & Questiaux 1989). Consequently, the approach of comparing IRSL and GLSL has been tested for the Raupo samples.

Bleaching characteristics and implications for dating

The aim of this set of experiments was to characterise the resetting behaviour of the IRSL, GLSL, and TL signals used for dating. Samples were bleached with the light by an Osram Ultra-Vitalux UV lamp (300 W) filtered through a Schott GG475 optical filter. The filter cuts off the light with wavelengths $\lambda < 475$ nm, thus giving a rough approximation of shallow water conditions.

The results of the bleaching experiments are shown in Fig. 5. It shows that the TL signals are less rapidly bleached in comparison to OSL. The two optical (IRSL, GLSL) and the two thermoluminescence (UV and violet blue) emissions show nearly identical bleaching characters. The similar resetting pattern of IRSL and GLSL was unexpected since the traps sampled from green light are presumably less easily bleachable. However, while this may apply to samples from other geological regions, it is obviously different for the sediments from Raupo.

Because the bleaching characteristics of IRSL and GLSL are nearly identical, comparison of IRSL and GLSL ages cannot be used to test for partial bleaching. Therefore, the approach of comparing luminescence signals with different bleaching characteristics is, at least for the Raupo samples, limited to OSL and TL.

As shown in Fig. 5, the light-sensitive TL signal is still not completely bleached after 105 s of light exposure under the simulated shallow water conditions. When considering that turbidity and turbulence will further severely reduce the light intensity within the water column, it is likely that zeroing the optical sensitive TL will take several days or more. Hence, complete bleaching of the TL from the Raupo samples is rather unlikely.

Fading test

One error source in dating is anomalous fading of the luminescence signal (Wintle 1973). Fading will result in age underestimation of the sample being dated. Storage tests were carried out for the Raupo samples to test if samples were affected by anomalous fading. Sets of subsamples were irradiated, stored for 4 weeks at room temperature, and subsequently pre-heated. The luminescence intensity was then monitored by repeated short shine measurements over a period of 1 yr. The signal loss by the short shine measurements and variability of photomultiplier sensitivity were corrected by measuring the intensity from natural subsamples. A plot of normalised luminescence intensity versus storage time is shown in Fig. 6. No significant changes in intensity with time have been observed and it is thus concluded that the Raupo samples are not affected by anomalous fading.

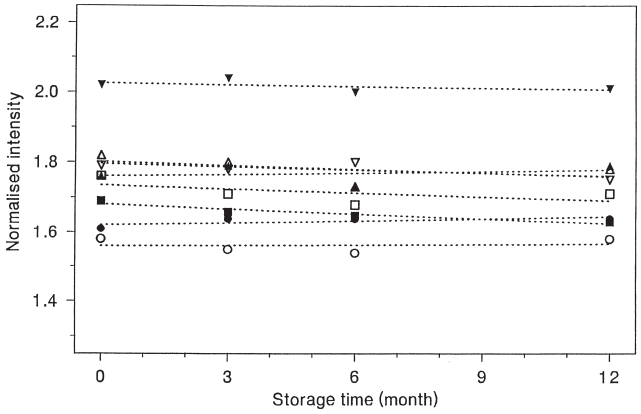

Fig. 6 Storage tests indicating the stability of the optically stimulated luminescence (OSL) signals used for dating.

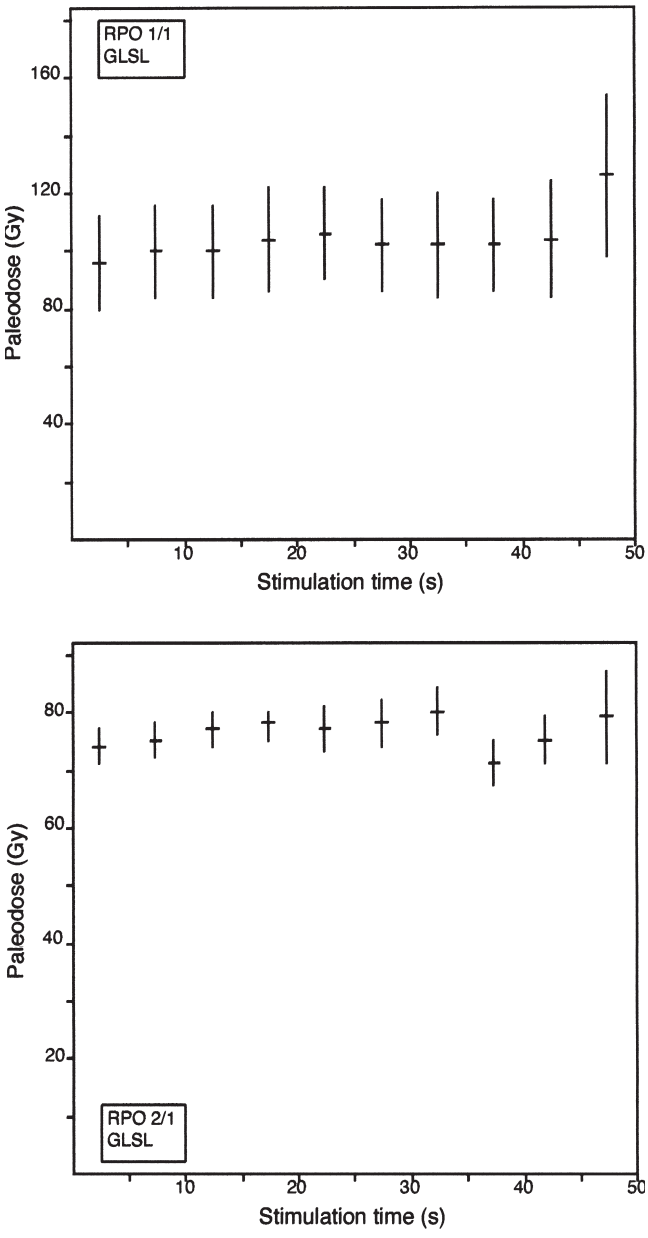

Fig. 7 Paleodose versus stimulation time (shine plateau test) for green light stimulated luminescence (GLSL) of samples RPO 1/1 and 2/1.

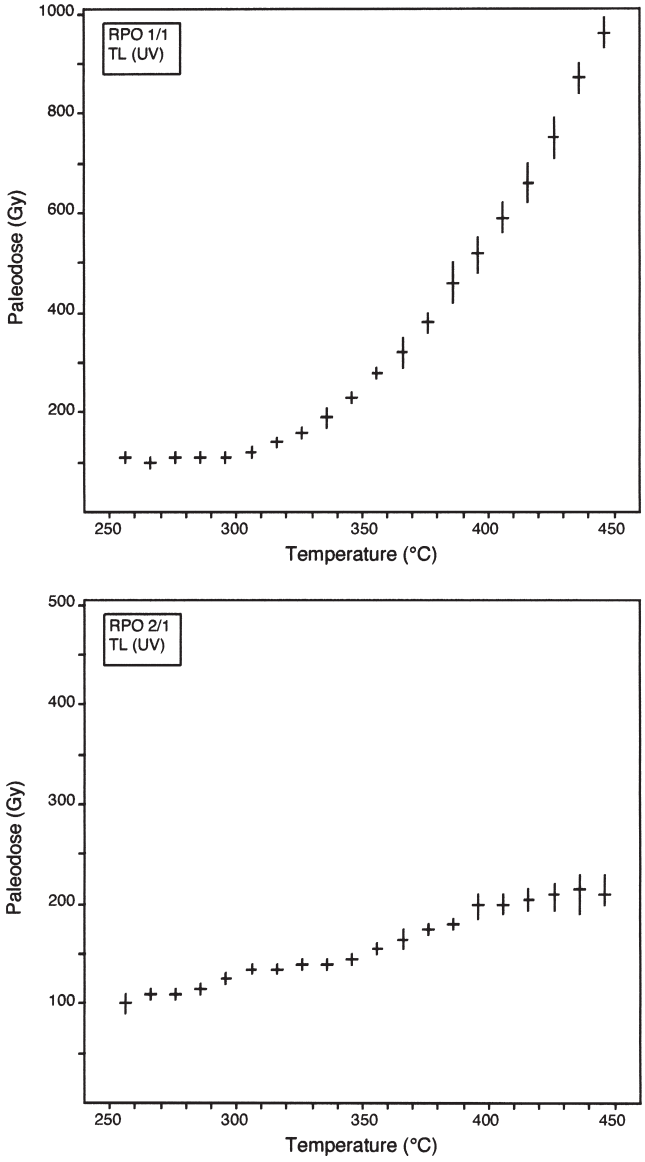

Fig. 8 Paleodose versus temperature (plateau test) for thermoluminescence (TL) (UV) of samples RPO 1/1 and 2/1.

Results and discussion of luminescence dating

Calculated ED and the resulting OSL and TL ages are summarised in Table 5. The OSL ages range between 18 700 ± 2200 and 26 000 ± 3800 yr. The TL ages are between 35 200 ± 5100 and 55 600 ± 10 000 yr. Shine plateaus, in a graph plotting paleodose versus stimulation time, are present for OSL (Fig. 7) while TL shows no plateaus above 300°C (Fig. 8). The absence of TL plateaus clearly indicates that the optically sensitive TL was not zeroed before deposition. Thus, the apparent TL age estimates have to be interpreted as maximum ages.

We assume zeroing of the OSL, as suggested by the shine plateaus (Fig. 7). It is concluded that the two sampled horizons were deposited within a short period of time, as indicated by the entire set of luminescence and radiocarbon ages. The apparent differences in the OSL age estimates are most likely caused by random scatter. Thus, we can calculate a weighted OSL age for the whole horizon, which is 21 700 ± 2600 yr ($\chi^2 = 5.6$).

CONCLUSIONS

Organic sediments of the Raupo complex were radiocarbon dated between 21 350 and 23 890 cal yr BP. The reliability of the ages is confirmed by the consistency of measurements on different organic fractions including organic residues, humic acids, and seeds. The ages for each different layer are consistent in themselves and are in stratigraphic order, with mean ages of 22 350 cal yr BP (layer A), 22 470 cal yr BP (layer B), 22 930 cal yr BP (layer C), and 22 960 cal yr BP (layer D).

Silty overbank deposits which alternate with the organic layers were dated with various luminescence techniques at a mean age of 21 700 ± 2600 yr. Both radiocarbon and OSL ages agree to an acceptable degree and it is thus concluded that both are suitable methods for dating similar sediments from Westland.

We interpret the Raupo complex to reflect a period of ameliorated climate during early Oxygen Isotope Stage 2 based on two observations:

(1) The energy change from outwash gravel deposits to fine grained silty overbank sediments produced the marked contrast between the Raupo complex and the gravels above and below. This change in sedimentation is directly related to the sediment supply of the Grey and Arnold Rivers. The fine-grained sediments of the Raupo complex have been deposited during a time of reduced river aggradation in comparison to the sedimentation of the Kumara-2_2 outwash gravel below. This abrupt change in sedimentation is interpreted to be a result of glacier retreat, which may relate to a significant change in climatic conditions.

(2) The growth of Cyperaceae and Juncaceae is evidenced by seeds in the organic layers. They are characteristic of a wetland environment with streambanks, river flats, swamps, and bogs because these plants need high watertables and nutrient-rich sediments to grow. The good preservation of Cyperaceae and Juncaceae in organic fine-grained sediment demonstrates low-energy sedimentation in the Raupo floodplain at the time of deposition.

The Kumara-2_2 advance of the Otira glaciation came to an end before 23 250–23 890 cal yr BP, as indicated by the radiocarbon ages of layer D of the Raupo complex. The radiocarbon ages of layer A (21 050–22 860 cal yr BP) date the end of the sedimentation of the fine-grained overbank sediments and give a maximum age for the deposition of the Kumara-3 outwash gravel.

At a broader scale, a climate amelioration at the same time is documented by ^{18}O and ^{13}C records from speleothems in the Mt Arthur region, northern South Island, New Zealand (Hellstrom et al. 1998). A negative excursion is documented in the ^{18}O record between 23 000 and 20 000 cal yr BP with values of only 0.6‰ above interglacial values and 0.4–0.9‰ below glacial values. Furthermore, the ^{13}C record of the speleothems shows a decline towards interglacial values at this time. The terrestrial Raupo complex and the Mt Arthur speleothem dataset agree well, indicating a climatic amelioration at least in New Zealand during Oxygen Isotope Stage 2 of the Last Glacial Maximum.

ACKNOWLEDGMENTS

Our sincere thanks go to Björn Andersen, Chris Hendy, and Thomas Lowell for their support in the field and for inspiring discussions; we thank Jane Shearer for organising contacts in New Zealand and for her hospitality during Anne's stay; cordial thanks go to Steve Reese and Markus Möll for collaboration and competent instructions in the radiocarbon laboratory. We thank Martin Suter and Georges Bonani for the use of the AMS facility at the Institute of Particle Physics of the ETH/PSI Zürich. We gratefully acknowledge that Janet Wilmshurst helped identify the seeds. Cordial thanks go to Pat Suggate, Susan Ivy-Ochs, and Meredith Kelly for several suggestions improving the manuscript. We also thank Peter Almond for his constructive review. The fieldwork was funded by the Swiss National Science Foundation project number 21-043469.95/1.

REFERENCES

Aitken, M. J. 1985: Thermoluminescence dating. London, Academic Press.

Aitken, M. J. 1992: Optical dating. *Quaternary Science Reviews 11*: 127–131.

Aitken, M. J. 1998: An introduction to optical dating. Oxford University Press.

Aitken, M. J.; Xie, J. 1992: Optical dating using infrared diodes: young samples. *Quaternary Science Reviews 11*: 147–152.

Andrée, M.; Oeschger, H.; Siegenthaler, U.; Riesen, T.; Moell, M.; Ammann, B.; Tobolski, K. 1986: ^{14}C dating of plant macrofossils in lake sediments. *Radiocarbon 28*: 411–416.

Bard, E.; Arnold, M.; Hamelin, B.; Tisnerat-Laborde, N.; Cabioch, G. 1998: Radiocarbon calibration by means of mass spectrometric $^{230}Th/^{234}U$ and ^{14}C ages of corals: an updated database including samples from Barbados, Mururoa and Tahiti. *Radiocarbon 40*: 1085–1092.

Barry, R. G.; Chorley, R. J. 1998: Atmosphere, weather & climate. London, Routledge.

Bonani, G.; Beer, J.; Hofmann, H.-J.; Synal, H.-A.; Wölfli, W.; Pfleiderer, C.; Kromer, B.; Junghaus, C.; Münnich, K. O. 1987: Fractionation, precision and accuracy in ^{14}C and ^{13}C measurements. *Nuclear Instruments and Methods 29*: 87–90.

Bøtter-Jensen, L.; Duller, G. A. T. 1992: A new system for measuring optically stimulated luminescence from quartz. *Nuclear Tracks and Radiation Measurements 20*: 549–553.

Bøtter-Jensen, L.; Ditlefsen, C.; Mejdahl, V. 1991: Combined OSL (infrared) and TL studies of feldspars. *Nuclear Tracks and Radiation Measurements 27*: 257–263.

Brennan, B. J.; Schwarcz, H. P.; Rink, W. J. 1997: Simulation of the gamma radiation field in lumpy environments. *Radiation Measurements 27*: 299–305.

Cheburkin, A. K.; Shotyk, W. 1996: An energy-dispersive miniprobe multielement analyzer (EMMA) for direct analysis of Pb and other trace elements in peats. *Fresenius Zeitschrift fuer Analytische Chemie 354*: 688–691.

Dansgaard, W.; Johnson, S. J.; Clausen, H. B.; Dahljensen, D.; Gundestrup, N. S.; Hammer, C. U.; Hvidbjerg, C. S.; Steffensen, J. P.; Sveinsbjörnsdottir, A. E.; Jouzel, J.; Bond, G. 1993: Evidence for general instability of past climate from a 250-kyr ice-core record. *Nature 364*: 218–220.

Denton, G. H.; Heusser, C. J.; Lowell, T. V.; Moreno, P. I.; Andersen, B. G.; Heusser, L. E.; Schlüchter, C.; Marchant, D. R. 1999: Interhemispheric linkage of paleoclimate during the last glaciation. *Geografiska Annaler 81 A*: 107–153.

Ditlefsen, C. 1992: Bleaching of K-feldspars in turbid water suspensions: a comparison of photo- and thermoluminescence. *Quaternary Science Reviews 11*: 33–38.

Duller, G. A. T. 1992: Comparison of equivalent doses determined by thermoluminescence and infrared stimulated luminescence for dune sands in New Zealand. *Quaternary Science Reviews 11*: 39–43.

Fairhall, A. W.; Schell, W. R.; Takashima, Y. 1961: Apparatus for methane synthesis for radiocarbon dating. *The Review of Scientific Instruments 32*: 323–325.

Frechen, M.; Schweitzer, U.; Zander, A. 1996: Improvements in sample preparation for the fine grain technique. *Ancient TL 14*: 15–17.

Fuller, I. C.; Wintle, A. G.; Duller, G. A. T. 1994: Test of partial bleach methodology as applied to the infrared stimulated luminescence of an alluvial sediment from the Danube. *Quaternary Geochronology (Quaternary Science Reviews) 13*: 539–543.

Geyh, M. A. 1983: Physikalische und Chemische Datierungsmethoden in der Quartärforschung. Clausthal-Zellerfeld, Ellen Pilger.

Geyh, M. A.; Krumbein, W. E.; Kudrass, H.-R. 1974: Unreliable ^{14}C dating of long-stored deep-sea sediments due to bacterial activity. *Marine Geology 17*: 45–50.

Gillespie, A.; Molnar, P. 1995: Asynchronous maximum advances of maritime and continental glaciers. *Revisions in Geophysics 33*: 311–364.

Goh, K. M.; Tonkin, P. J.; Rafter, T. A. 1978: Implications of improved radiocarbon dates of Timaru peats on Quaternary loess stratigraphy. *New Zealand Journal of Geology and Geophysics 21*: 463–466.

Hajdas, I. 1993: Extension of the radiocarbon calibration curve by AMS dating of laminated sediments of lake Soppensee and lake Holzmaar. Diss. ETH Nr. 10157, Zürich.

Hammond, A. P.; Goh, K. M.; Tonkin, P. J.; Manning, M. R. 1991: Chemical pretreatments for improving the radiocarbon dates of peats and organic silts in a gley podzol environment: Graham's terrace, north Westland, New Zealand. *New Zealand Journal of Geology and Geophysics 34*: 191–194.

Hellstrom, J.; McCulloch, M.; Stone, J. 1998: A detailed 31,000-year record of climate and vegetation from the isotope geochemistry of two New Zealand speleothems. *Quaternary Research 50*: 167–178.

Huntley, D. J.; Godfrey-Smith, D. I.; Thewalt, M. L. W. 1985: Optical dating of sediments. *Nature 313*: 105–107.

Johnson, S. J.; Clausen, H. B.; Dansgaard, W.; Fuhrer, K.; Gundestrup, N.; Hammer, C. U.; Iverson, P.; Jouzel, J.; Stauffer, B.; Steffensen, J. P. 1992: Irregular glacial interstadials recorded in a new Greenland ice core. *Nature 363*: 311–313.

Kigoshi, K.; Suzuki, N.; Shiraki, M. 1980: Soil dating by fractional extraction of humic acid. *Radiocarbon 22*: 853–857.

Kitagawa, H.; van der Plicht, J. 1998: A 40,000-year varve chronology from Lake Suigetsu, Japan: extension of the radiocarbon calibration curve. *Radiocarbon 40*: 505–515.

Krause, W. E.; Krbetschek, M. R.; Stolz, W. 1997: Dating of Quaternary lake sediments from the Schirmacher Oasis (East Antarctica) by infra-red stimulated luminescence (IRSL) detected at the wavelength of 560 nm. *Quaternary Geochronology (Quaternary Science Reviews) 16*: 387–392.

Krbetschek, M. R.; Götze, J.; Dietrich, A.; Trautmann, T. 1997: Spectral information from minerals relevant for luminescence dating. *Radiation Measurements 27*: 695–748.

Loosli, H.-H.; Heimann, M.; Oeschger, H. 1980: Low-level gas proportional counting in an underground laboratory. *Radiocarbon 22*: 461–469.

Mook, W. G.; Streurman, H. J. 1983: Physical and chemical aspects of radiocarbon dating. *In*: Mook, W. G.; Waterbolk, H. J. *ed*. Proceedings of the 1st International Symposium ^{14}C and Archaeology, Vol. PACT, 8. Councile Europe, Strasbourg. Pp. 31–55.

Neftel, A.; Oeschger, H.; Staffelbach, T.; Stauffer, B. 1988: CO_2 record in the Byrd ice core 50,000–5,000 years BP. *Nature 331*: 609–611.

Nelson, C. S.; Cooke, P. J.; Hendy, C. H.; Cuthbertson, A. M. 1993: Oceanographic and climatic changes over the past 160,000 years at deep sea drilling project site 594 off southeastern New Zealand, Southwest Pacific Ocean. *Paleoceanography 8*: 435–458.

Olsson, I. U. 1986: A study of errors in ^{14}C dates of peats and sediment. *Radiocarbon 28*: 429–435.

Pillans, B.; McGlone, M.; Palmer, A.; Mildenhall, D.; Alloway, B. V.; Berger, G. 1993: The Last Glacial Maximum in central and southern North Island, New Zealand: a paleoenvironmental reconstruction using the Kawakawa Tephra Formation as a chronostratigraphic marker. *Palaeogeography, Palaeoclimatology, Palaeoecology 101*: 283–304.

Prescott, J. R.; Robertson, G. B. 1997: Sediment dating by luminescence: a review. *Radiation Measurements 27*: 893–922.

Preusser, F. 1999a: Lumineszenzdatierung fluviatiler Sedimente - Fallbeispiele aus der Schweiz und Norddeutschland. *Kölner Forum für Geologie und Paläontologie 3*. 62 p.

Preusser, F. 1999b: Luminescence dating of fluvial sediments and overbank deposits from Gossau, Switzerland: fine grain dating. *Quaternary Geochronology (Quaternary Science Reviews) 18*: 217–222.

Preusser, F. 1999c: Bleaching characteristics of some optically stimulated luminescence signals. *Ancient TL 17*: 11–14.

Preusser, F.; Kasper, H. U. 2001: Comparison of dose rate determination using high-resolution gamma spectrometry and inductively coupled plasma-mass spectrometry. *Ancient TL 19*: 17–21.

Preusser, F., Müller, B. U.; Schlüchter, C. 2001: Luminescence dating of sediments from the Luthern Valley, central Switzerland, and implications for the chronology of the last glacial cycle. *Quaternary Research 55*: 215–222.

Spooner, N. A.; Questiaux, D. G. 1989: Optical dating—Achenheim beyond the Eemian using green and infra-red stimulation. Long and short range limits in luminescence dating. *Oxford Research Laboratory for Archaeology and the History of Art Occasional Publication 9*: 97–103.

Sposito, G. 1989: The chemistry of soils. Oxford, Oxford University Press.

Steinmann, P.; Shotyk, W. 1997: Chemical composition, pH and redox state of sulphur and iron in complete vertical pore water profiles from two sphagnum peat bogs, Jura Mountains, Switzerland. *Geochimica et Cosmochimica Acta 61 (6)*: 1143–1163.

Stuiver, M.; Reimer, P. 1999: 1999 CALIB [Computer program] URL http://depts.washington.edu/qil/

Stuiver, M.; Reimer, P. J.; Bard, E.; Beck, J. W.; Burr, G. S.; Hughen, K. A.; Kromer, B.; McCormac, G.; van der Plicht, J.; Spurk, M. 1998: INTCAL98 Radiocarbon age calibration, 24,000–0 cal BP. *Radiocarbon 40*: 1041–1083.

Suggate, R. P. 1965: Late Pleistocene geology of the northern part of the South Island, New Zealand. *New Zealand Geological Survey Bulletin 77*.

Suggate, R. P. 1990: Late Pleistocene and Quaternary glaciations of New Zealand. *Quaternary Science Reviews 9*: 175–197.

Suggate, R. P.; Moar, N. T. 1970: Revision of the chronology of the Late Otira Glacial. *New Zealand Journal of Geology and Geophysics 13*: 742–746.

Törnqvist, T. E.; de Jong, A. F. M.; Oosterbaan, W. A.; van der Borg, K. 1992: Accurate dating of organic deposits by AMS ^{14}C measurement of macrofossils. *Radiocarbon 34*: 566–577.

Weiss, D.; Shotyk, W.; Cheburkin, A. K.; Gloor, M. 1998: Determination of Pb in ashed peat and plants using an energy dispersive miniprobe multielement analyzer (EMMA). *Analyst 123*: 2097–2102.

White, J. W. C.; Ciais, P.; Figge, R. A.; Kenny, R.; Markgraf, V. 1994: A high-resolution record of atmospheric CO_2 content from carbon isotopes in peat. *Nature 367*: 153–156.

Williams, P. W. 1996: A 230 ka record of glacial and interglacial events from Aurora cave, Fiordland, New Zealand. *New Zealand Journal of Geology and Geophysics 39*: 225–241.

Wintle, A. G. 1973: Anomalous fading of thermoluminescence in mineral samples. *Nature 245*: 143–144.

Wintle, A. G. 1997: Luminescence dating: laboratory procedures and protocols. *Radiation Measurements 27*: 769–817.

Wohlfarth, B.; Skog, G.; Possnert, G.; Holmqvist, B. 1998: Pitfalls in the AMS radiocarbon-dating of terrestrial macrofossils. *Journal of Quaternary Science 13*: 137–145.

Zbinden, H.; Andrée, M.; Oeschger, H.; Ammann, B.; Lotter, A.; Bonani, G.; Wölfli, W. 1989: Atmospheric radiocarbon at the end of the Last Glacial: an estimate on terrestrial macrofossils from lake sediments. *Radiocarbon 31*: 795–804.